Efficiency of *Alstonia schoalris* Leaves on Mild Steel in Acid Medium as Pickling Inhibitor

P.K. Neena[*], N. Poongothai and P.R. Abhirami

Department of Sciences, Amrita School of Engineering, Amrita Vishwa Vidyapeetham, Coimbatore-641112, India

*Corresponding author: E-mail: neenamurali77@gmail.com; npgothai@gmail.com

This work aims to find the inhibition efficiency of *Alstonia schoalris* leaves on mild steel in 1N HCl medium. Corrosion monitoring was done using weight loss method, potentiodynamic polarization studies like Tafel and impedance studies and the results shows that the inhibitor acts well on mild steel in acidic medium. Polarization studies show that the inhibitor behaves like a mixed type. The inhibitor was characterized using FTIR which showed the presence of hetero atoms in the inhibitor molecule that get adsorbed on metal surface and provided better efficiency and that was proven by different adsorption isotherm. Zeta potential showed the stability of particle in the medium. Surface analysis of specimen was studied using FESEM, EDX and contact angle measurements. The analysis showed that the surface exposed to inhibitor is less corroded and contact angle measurement showed hydrophilic nature of the surface.

Keywords: *Alstonia scholaris*, Corrosion rate, Inhibition efficiency, Mild steel.

INTRODUCTION

Mild steel is widely used as the constructional material in most of the industries particularly in food, petroleum, power production, chemical and electrochemical industries, especially due to its excellent mechanical properties and low cost. The major problems of steel is its dissolution in alkaline and acidic medium [1-4]. Corrosion of mild steel in acidic and aqueous solutions is one of the major areas of concern in the industries where in acids are widely used for applications such as acid pickling, acid descaling, *etc.* [5,6]. Because of this general aggressiveness of acid solution towards such engineering metals they are being corroded easily. Now, it is our responsibility to find an easy and best way of corrosion protection.

Use of paint and/or polymer as a protective coating, pickling, wrapping with vapour phase inhibitor coated paper, galvanizing, *etc*. are some of the methods [7-10] to protect the material from corrosion. Depending on the requirements of different methods are being applied in different situations. Pickling is used in industrial applications, where the metal is introduced into pickle liquor in order to obtain a clean surface. Generally, strong acids are chosen as the pickle liquor [11]. Compounds, generally known as inhibitors are added to this liquor to avoid unexpected metal loss and acid consumption. However, toxicity

is the matter of concern for these chemical inhibitors like certain inorganic or heterocyclic organic compounds *viz.* indoles, benzotriazoles, ammonium benzoates, pyrimidothiazines, aromatic hydrazides, thiocarbanilide, poly(vinyl alcohol-cysteine), S-allyl-O,O-dialkyldithiophosphates, benzonitrile, poly(vinyl alcohol-*o*-methoxy aniline), L-cysteine methyl ester hydrochloride, substituted arsine and phosphines, thiourea and their derivatives, amino acids, S-alkylisothiouranium iodide, valeronitrile, formaldehyde, ethoxylated fatty amines, fatty acids, oxadiazoles, *etc*. are reported as inhibitors in the literature [12-30].

Scientists have now turned their attentions to different kinds of natural, synthetic but non-toxic and green extracts such as *Theobroma cacao* peels, *Gentiana olivieri*, *Alstonia scholaris* bark, *Primula vulgaris* flower, Gorse aqueous extract, henna, natural honey, *Azadirachta indica* (neem), *Pongamia glabra*, *Annona squamosa*, *Solanum trilobatum*, *Sapindus trifoliatus*, *Acacia concinna*, herbal triphala, *Nerium odorum* flower and its leaves, *Emblica officinalis*, *Terminalia bellirica*, *Terminalia chebula*, *Calotropis gigantea* latex, *Swertia angustifolia*, Eucalyptus leaves, *Rosmarinus officinalis*, tannins extracts from acacia and fine barks, pomegranate alkaloids, cashew juice inhibitors, *etc*. have been used as inhibitor for corrosion protection of metallic surfaces [31-51].

The initial empirical approaches for the selection of the inhibitor were followed by more scientific approaches in the selection and design of the inhibitors [52]. The basic action of inhibitor is attributed to an increase in over voltage of hydrogen ion discharge as the cathodic reaction of corrosion process or an increase in ohmic resistance of an inhibitor film at the metal-electrolyte interface or due to some type of adsorption on the metal surface [53]. The strength of adsorption bond depends upon the electron density on the donor atom of the functional group and polarizability of group. The extracts of some common plants and byproducts contain different organic compounds such as amino acids, alkaloids and tannins. Most of these constituents are known to have inhibitive action. It is therefore, to be expected that these compounds would exert a retarding action on the dissolution of base metals and would then find applications in the acid pickling of composite systems [54]. So organic compounds in natural products containing hetero atoms are found to have higher basicity and electron density and this assists in corrosion inhibition. Due to ecofriendly, biodegradability, cost-effectiveness, less-toxicity and easy availability of these products, the trends of using them have become increasingly important in the recent years. The important factors influencing corrosion inhibition are the nature of bonding and the effect of structure of adherent compound on the strength and stability of bond, paves the way to the concept of 2D quasi-compounds [55]. This work aims to find the inhibitory action of *Alstonia scholaris* leaves on mild steel (MS) in 1N HCl.

EXPERIMENTAL

Preparation of specimens: From a sheet of mild steel with the composition, carbon 0.06 %, manganese 0.4 %, silicon 0.05 %, phosphorus 0.03 %, sulphur 0.0277 %, chromium 0.022 %, molybdenum 0.014 % and nickel 0.0117 %; coupons of 5 cm × 1 cm were cut. The specimens were polished using different grades of emery paper, washed with tap water, followed by distilled water, dried and stored and then used for the present studies.

Preparation of extract: The plant *Alstonia schoalris* leaves were collected from farm house premises; shadow dried to avoid too many chemical changes and was powdered. The extract was prepared by taking 25 g of powdered sample in 250 mL of 1 N HCl, refluxed for 3 h and kept overnight, filtered and made up to 500 mL using the same acid.

Gravimetric analysis: The mild steel specimens of known weight and area were immersed in a 100 mL beaker containing the test solutions at room temperature for various immersion periods like 0.5, 1, 3, 6 and 24 h in doublets. A beaker containing the same volume of acid was kept as reference. After the respective time period, the specimens were removed from the medium, weighed and the weight loss (W) was recorded as the weight difference of the specimen before and after immersion. From the weight loss, corrosion rate (C.R.) (eqn. 1) and inhibition efficiency (I.E.) (eqn. 2) were calculated as:

$$C.R. = \frac{534 \times W}{DAT} \tag{1}$$

where, W= weight loss in mg, D = density of metal (7.9 g/cc), A = area of exposure in cm^2 and T = time of exposure in hours.

$$I.E. = \frac{W_0 - W}{W_0} \times 100 \tag{2}$$

where, W_0 = weight loss of specimen without inhibitor, W = weight loss of specimen with inhibitor.

Same analysis was carried out as the same procedure of room temperature at elevated temperatures *viz.* 313, 323, 333, and 343 K for an immersion period of 0.5 h to understand the influence of temperature on inhibition. From the results obtained, thermodynamic parameters like activation Energy(E_a), free energy change (ΔG), enthalpy (ΔH) and entropy change (ΔS) were calculated and nature of the process were elucidated.

Potentiodynamic polarization studies: Polarization studies were carried out using CH 660 electrochemical work station. Conventional, three electrode assembly of platinum as the auxillary electrode, SCE as reference and mild steel as the working electrode. The studies were carried out in inhibitor concentrations from 6 to 10 % in 1N HCl at room temperature. The working electrode was kept in the test solution for 15 min to obtain the constant potential. The studies were carried out at a scan rate of 0.01 mV/s in a potential range of - 1 V to + 1 V. The linear anodic and cathodic curves are extrapolated to obtain the corrosion current (I_{corr}) and potential (E_{corr}) and anodic (b_a) and cathodic (b_c) slopes and inhibition efficiency (I.E.) were determined using eqn. 3.

$$I.E. = \frac{I_{blank} - I}{I_{blank}} \times 100 \tag{3}$$

Electrochemical impedance spectroscopy (EIS): EIS studies were carried out using CH 660 electrochemical work-station. The working electrode was immersed in test solution for 30mins to attain a constant potential. Then using the three electrode assembly, mild steel as working electrode, SCE as reference and platinum as auxillary electrode were used. AC sine wave of 0.005 V amplitude with frequency 10000 Hz to 0.1 Hz was used. Using Nyquist plot charge transfer resistance (R_{ct}), double layer capacitance (C_{dl}) values were found out from which inhibition efficiency (I.E.) was determined.

The FTIR spectra were recorded by using FTIR spectrophotometer IR PRESTIGE 21, Shimadzu instrument from the range of 4000-500 cm^{-1} using KBr pellets. XRD spectrum of powdered sample was recorded using Shimazdu instrument; CuK$_\alpha$ radiation (λ = 1.5418 Å) was used. Zeta potential of inhibitor was analyzed in order to analyze the stability of particle in medium. It was measured using Zetasizer Ver. 6.32, USA. FESEM images of mild steel specimen immersed in pickling medium with and without inhibitor were recorded using ZEISS SIGMA instrument. EDX analysis of mild steel specimen exposed to only inhibitor was carried out using ZEISS SIGMA instrument in order to elucidate the major elements present on the surface.

The contact angle measurement showed the wettability of the surface. The contact angle photographs for blank specimen, specimen exposed to optimum concentration (8 %) and only inhibitor was recorded using the instrument HO-IAD-CAM 01.

RESULTS AND DISCUSSION

Gravimetric analysis: The corrosion rate (C.R.) and inhibition efficiency (I.E.) of mild steel in 1 N HCl in different

concentrations of inhibitor for various time periods of immersion is represented in Figs. 1 and 2. It is visible that with concentration of inhibitor inhibition efficiency increases upto an optimum concentration and then slightly decreases. At room temperature the range of concentration which showed highest I.E. at various time are from 7 to 9 %. The maximum I.E. obtained was 98 % at a concentration of 8 % at 0.5 h. The inhibition action can be attributed to adsorption of inhibitor molecules on the metal surface. It is also evident that with increase in time of immersion also inhibition efficiency decreases. This may be because when concentration increases the completion among molecules to occupy active sites increases as a result the efficiency shows a decrease [56,57].
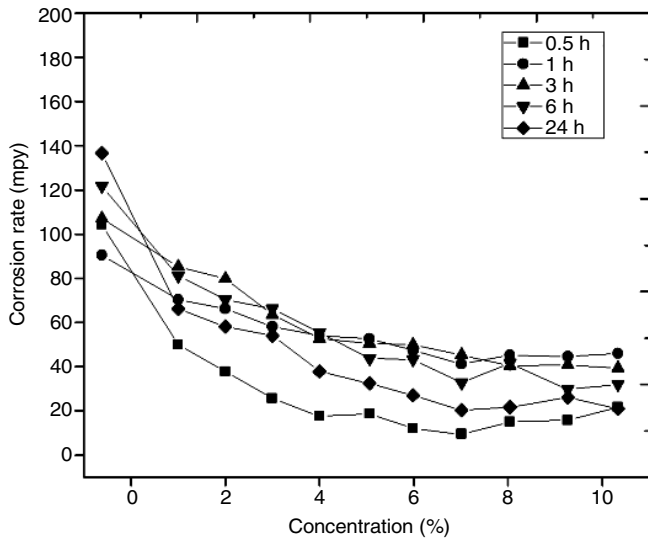
Fig. 1. Corrosion rate as a function of inhibitor concentration for mild steel in 1 N HCl at room temperature
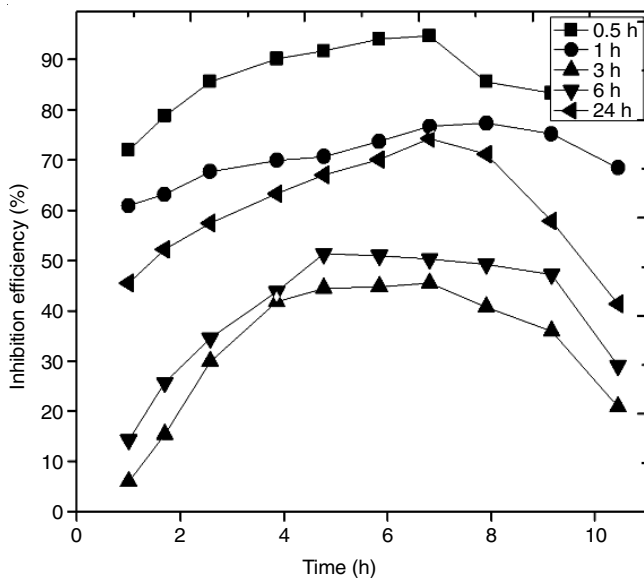
Fig. 2. Inhibition efficiency as a function of time for mild steel in 1 N HCl at room temperature

Weight loss studies at elevated temperatures (313, 323, 333 and 343 K) are carried out and results are depicted in Fig. 3. This shows that at elevated temperatures, inhibition efficiency decreases. This may be because at elevated temperature the
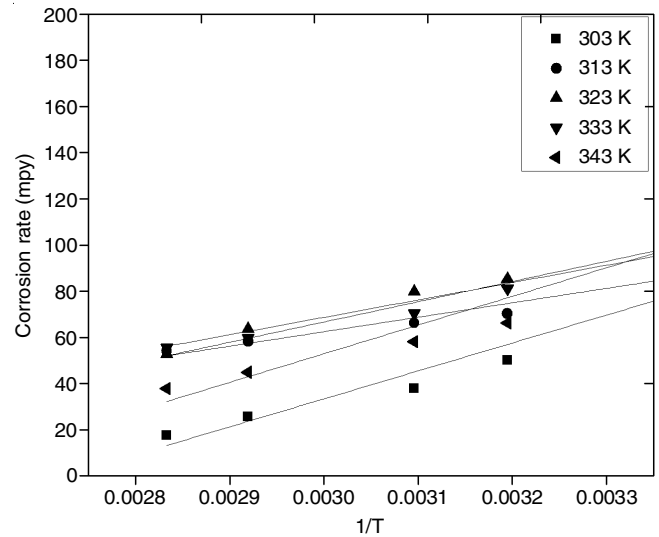
Fig. 3. Corrosion rate as a function of inverse of temperature for mild steel immersed in various inhibitor concentrations at different temperatures

kinetic energy of molecules increases which increase the rate of desorption and thus corrosion rate increases. In other words, this observation may be due to the degradation of active groups in inhibitor at higher temperatures [56,58].

Thermodynamic parameters: A plot between log C.R. *vs.* 1/T is shown in Fig. 4. From the slope of plot, activation energy (E_a) is calculated using eqn. 4 and the results are depicted in Table-1.
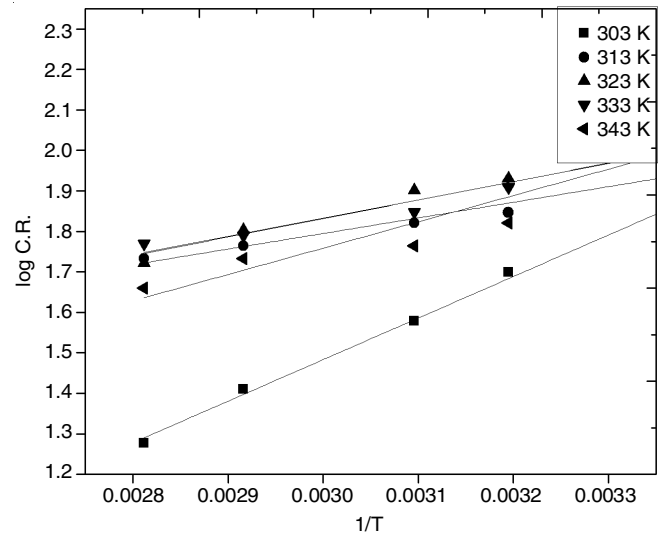
Fig. 4. Arrhenius plot for mild steel in various concentrations of inhibitor at different temperature

TABLE-1
ACTIVATION ENERGY, ENTHALPY AND ENTROPY
CHANGE VALUES FOR INHIBITOR ON MILD STEEL IN
1 N HCl AT VARIOUS TEMPERATURES

Temp. (K)	E_a (kJ/K/mol)	ΔH (kJ/mol)	ΔS (kJ/mol)
303	72931.394	-20.0107	-2727.4574
313	79348.522	-30.9766	-5239.3300
323	96789.235	-37.4277	-4399.8870
333	1.13×10^5	-24.3325	-7815.4232
343	2.10×10^5	-11.2185	1679.1880

$$E_a = 2.303 \times R \times slope \qquad (4)$$

The results show that at higher temperature more energy is needed to cross the energy barrier which shows less inhibition at higher temperature. Free energy change (ΔG) for each concentration of inhibitor is calculated using the eqn. 5 and results are shown in Table-2.

$$\Delta G = 2.303 \, RT \, (1.74 + \log (\theta/1 - \theta) - \log C \qquad (5)$$

where, R = universal gas constant (J/K/mol), θ = surface coverage, C = concentration.

TABLE-2
FREE ENERGY CHANGE VALUES FOR MILD STEEL EXPOSED TO DIFFERENT CONCENTRATIONS OF INHIBITOR IN 1 N HCl

Conc. (%)	Free energy change (ΔG) (kJ/mol)				
	303 K	313 K	323 K	333 K	343 K
Blank	-10.0947	-10.4279	-10.7611	-10.9029	-11.4274
1	-12.4694	-17.5743	-9.54091	-12.5097	-17.4858
2	-11.6533	-16.0199	-9.7171	-12.6126	-16.2713
3	-11.8177	-15.4841	-11.6998	-12.0819	-15.4972
4	-12.1802	-15.0081	-12.3320	-12.6728	-16.3069
5	-9.9587	-14.5221	-10.8806	-17.3769	-16.2892
6	-10.0713	-14.4367	-11.5702	-12.9851	-16.4562
7	-12.4508	-14.4558	-14.2080	-10.4538	-17.0344
8	-9.3464	-12.9312	-11.9233	-8.5641	-15.1127
9	-8.6131	-13.5879	-10.4812	-13.5461	-11.2188
10	-9.2824	-12.4402	-7.1846	-9.6371	-10.0032

The negative value of ΔG shows exothermic and spontaneous nature of adsorption. From the plot of ΔG *vs.* 1/T, slope gives ΔH and intercept gives ΔS values. The negative value of ΔH shows exothermic nature of the process. The high values of E_a corresponding to ΔH value show the involvement of gaseous evolution reaction, here typically hydrogen gas evolution during the process. Negative values of ΔS shows that the reaction happens through an associative mechanism. The association of adsorbent and adsorbate through an activated complex and decreases the disorderness. The positive value of entropy at high temperature show high randomness which can be because of increased kinetic energy of molecules and thus reduces the inhibition efficiency. This result is highly coherent with the obtained results of gravimetric analysis at elevated temperatures. It can be inferred that the inhibition action is more prominent at room temperature or slightly higher temperature but poor at higher temperature.

Potentiodynamic polarization studies: Potentiodynamic polarization studies for mild steel in 1N HCl with and without inhibitor was carried out, Tafel plots were studied and parameters like corrosion current (I_{corr}), corrosion potential (E_{corr}), cathodic slope (b_c), anodic slope (b_a) and inhibition efficiency were determined and represented in Table-3 and Fig. 5. The decreased I_{corr} value on addition of inhibitor shows the inhibition action by the adsorption of molecule on the metal surface. It is also evident from the change in both anodic and cathodic slope values that the inhibitor has considerable effect on both anodic and cathodic reaction. An inhibitor can only be classified as anodic or cathodic inhibitor only if there is a change of 85 mV/SCE with respect to the blank. So, it is clear that the inhibitor behaves like a mixed- type. When the concentration of inhibitor was increased from 6 % to 10 %, inhibition efficiency

TABLE-3
TAFEL PARAMETERS FOR DIFFERENT CONCENTRATIONS OF INHIBITOR FOR MILD STEEL IN 1 N HCl AT ROOM TEMPERATURE

Conc. (%)	Cathodic slope (b_c)	Anodic slope (b_a)	E_{corr} (V)	I_{corr} (A)	I.E. (%)
Blank	6.972	10.883	-0.433	4.675×10^{-4}	–
6	6.709	9.700	-0.437	2.008×10^{-4}	57.04
7	5.072	11.690	-0.419	2.157×10^{-4}	53.86
8	5.559	13.958	-0.399	1.189×10^{-4}	74.57
9	4.331	11.083	-0.426	1.313×10^{-4}	71.91
10	5.174	13.834	-0.400	1.337×10^{-4}	71.40
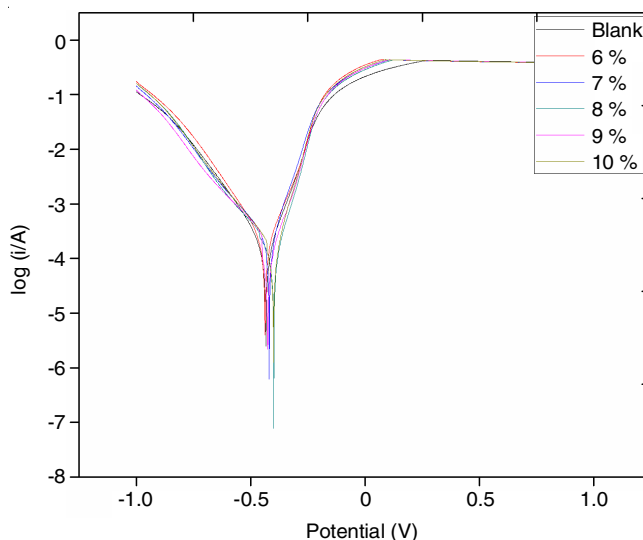
Fig. 5. Tafel plot at room temperature for mild steel in 1 N HCl at room temperature

increased from 53 % to 74 % and maximum inhibition efficiency was shown at the optimum concentration of 8 %. The inhibition efficiency obtained from polarization studies are less than that obtained from weight loss measurement. This may be because polarization studies are carried out in a quick time span. This time may not be sufficient for the inhibitor molecule to adsorb on the metal surface and hence inhibition efficiency showed a decrease when compared to weight loss method where the probability of gradual adsorption is more [59].

Electrochemical impedance spectroscopy (EIS): Impedance measurement has been carried out in order to evaluate charge transfer capacitance (R_{ct}) and double layer capacitance (C_{dl}) and inhibition efficiency (I.E.). Fig. 6 represents Nyquist plots of mild steel specimens in 1 N HCl in various concentrations of inhibitor and the evaluated parameters are depicted in Table-4.

TABLE-4
PARAMETERS CALCULATED FROM NYQUIST PLOT FOR MILD STEEL IN 1 N HCl FOR VARIOUS CONCENTRATIONS OF INHIBITOR

Conc. (%)	R_{ct} (ohm cm^2)	C_{dl} (F cm^{-2})	I.E. (%)
Blank	23.63	0.000249	–
6	83.55	7.047×10^{-5}	71.71
7	79.44	8.123×10^{-5}	70.25
8	165.30	3.432×10^{-5}	85.70
9	146.50	4.016×10^{-8}	83.87
10	110.45	5.428×10^{-5}	78.20
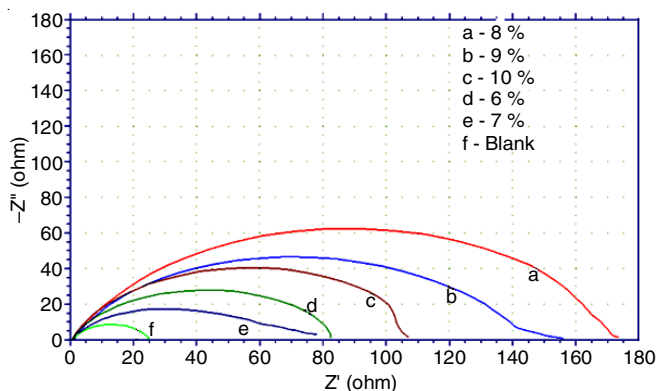
Fig. 6.   Nyquist plot for mild steel in different inhibitor concentrations in 1 N HCl at room temperature

The electrochemical parameters for the system were evaluated using ZSimpWin software. The given circuit [(((R(C(R (Q (RW))))(CR)))] showed excellent correlation with the obtained results. Fig. 6 shows semicircular appearance, indicating that the process of mild steel corrosion is mainly controlled by charge transfer. Deviation from the appearance may be due to the inhomogenity of metal surface arising from surface roughness. Introduction of inhibitor has decreased C_{dl} values indicating the adsorption of molecules on the surface. The lowest capacitance and highest resistance and inhibition efficiency values were obtained for the optimum concentration 8 %. Thus, the results obtained were in agreement with weight loss and Tafel studies.

Mechanism of inhibition: The inhibitory action by the molecules is expected to be by its adsorption on the metal surface. The components present in the inhibitor are alkaloids, flavanoids and tannins. The main constituents present are alstonamine, rhaximanine, erythrodiol and uvaol [60]. In acidic medium, the metal surface will be positively charged. The molecules get adsorbed on the electroactive sites on metal by the electrostatic interaction of lone pair of electrons on hetero-atom of molecules and positive metal surface. There are several compounds present in the inhibitor, and the inhibition action is a synergetic effect of all components present. The surface coverage values (θ) were determined from the weight loss results and efforts were done to fit the values into different isotherms. The values followed Langmuir adsorption isotherm which gives a linear fit for the plot between log (θ/1 − θ) *vs.* log C. Adsorption isotherm was studied at 0.5 and 24 h to know the nature of adsorption on prolonged exposure. At both the time of immersion, the data fitted with R^2 value of 0.97 and 0.98, respectively. This shows that the adsorption is monolayer physisorption even at higher time of immersion.

XRD analysis: Fig. 7 shows the powder XRD pattern of the inhibitor. Three prominent peaks were observed at 2θ values of 14.9º, 24.3º and 30º; and these Braggs reflections clearly indicated that presence of (100), (012) and (210) sets of lattice planes respectively. It fairly high intense peak at these values. The observed peak broadening and noise were probably responsible of macromolecules present in the plant extract. Hence, XRD pattern thus clearly illustrated that the crystalline macrosize particles like alstonamine, rhaxamine, erythrodiol, uvaolpresent in the plant extract. In addition to the Bragg peaks representative, additional yet unassigned peaks are also observed
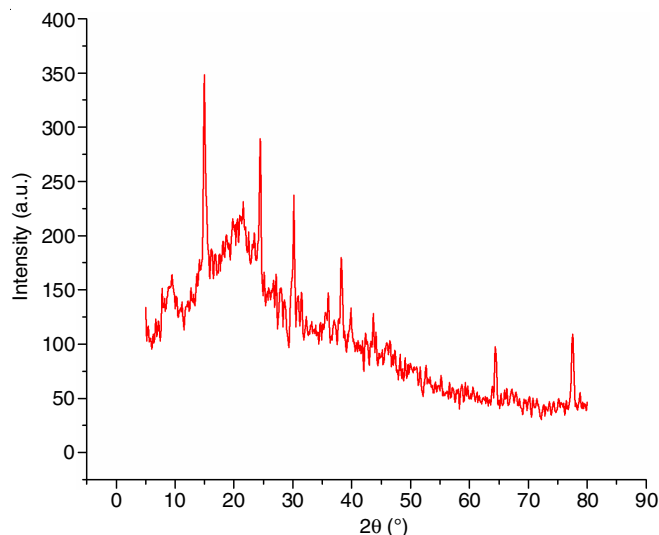
Fig. 7. XRD pattern of the inhibitor

suggesting that the crystallization of bioorganic phase occurs on the surface. The line broadening of the peaks is primarily due to small particle size.

FTIR analysis: The broad peak at 3000 cm⁻¹ show O-H vibration peaks, the peak at 1600 cm⁻¹ shows alkene C-H vibrations and peak at 1400 cm⁻¹ show aromatic ring C-C vibrations, peak at 700 cm⁻¹ shows O-H out of plane bending vibrations and N-H bending vibrations are reflected in the peak at 600 cm⁻¹ (Fig. 8). These values show the presence of heteroatoms in the inhibitor molecules [61].
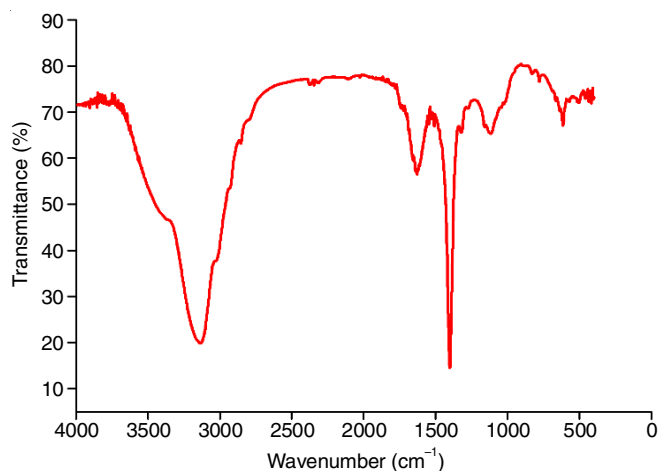
Fig. 8. FTIR spectrum of the inhibitor

Zeta potential and particle size distribution: Zeta potential is the measure between boundary and diffuse layer. This in turn measures the surface charge and stability of the particle in the medium. It can be taken as the direct measure of particle size. If the size of particle is less the stability will be more and if the particle has an increased size; it shows less zeta potential value indicating the unstability of particle in the medium. Zeta potential of the inhibitor was measured and was found to be -8.06 mV (Fig. 9a). This shows that the dispersed particles in the medium is highly unstable (Fig. 9b). It can be inferred that this unstability can be aided to adsorption of these molecules on to the metal surface.
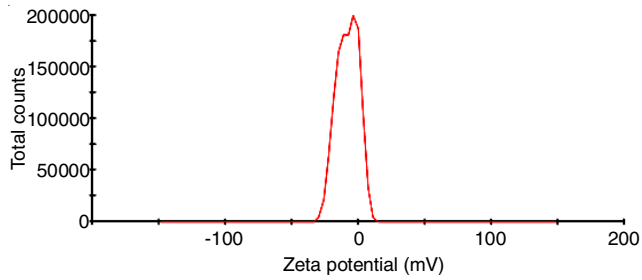
Fig. 9a. Zeta potential of the inhibitor
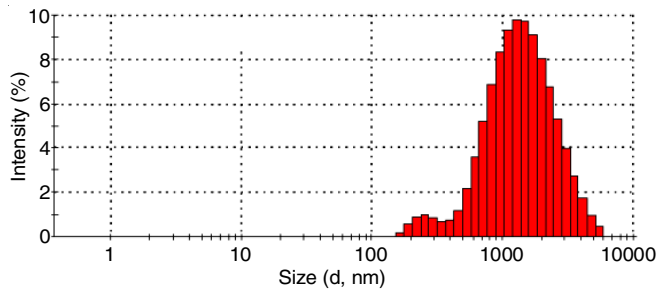
Fig. 9b. Particle size distribution of the inhibitor

FESEM analysis: FESEM images of mild steel specimens is exposed to the pickling medium with and without inhibitor are shown in Fig. 10. The specimen exposed to the pickling liquor shows a rough and corroded texture than exposed with inhibitor. The image of sample exposed to the optimum concentration and only inhibitor shows a comparatively smooth

surface, which shows reduced rate of corrosion due to adsorption of inhibitor molecules on the surface.

Energy dispersive X-ray spectroscopy (EDX): Fig. 11 shows that Fe, O and Cl were found to be the major elements present in the extract. In all these compounds, iron and oxygen presented as high concentration of 65 and 36 %, respectively. The iron present is due to metal surface and oxygen, due constituent in inhibitor. The EDX spectrum and weight percentage of elements obtained are represented in Table-5.

TABLE-5
WEIGHT (%) OBTAINED FROM EDX SPECTRUM

Element	Weight (%)	Atomic (%)
O K	31.59	61.18
Cl K	2.72	2.38
Fe K	65.69	36.45
Total	100.00	

Contact angle: Contact angle measurement was carried out to find the nature of the surface using Sessile drop method. If the measured angle gives value of 0-45º, surface is wettable and hydrophilic in nature. If angle is 90º, the surface is moderately wettable and completely non-wettable at 180º [62]. The images show the lowest contact angle for the blank specimen of 15º. The specimen which was exposed to optimum concentration yielded an angle of 21º and that of only inhibitor was 29º. Both are below 45º showing the surface to be hydrophilic in nature. The corresponding interfacial tension (IFT) values
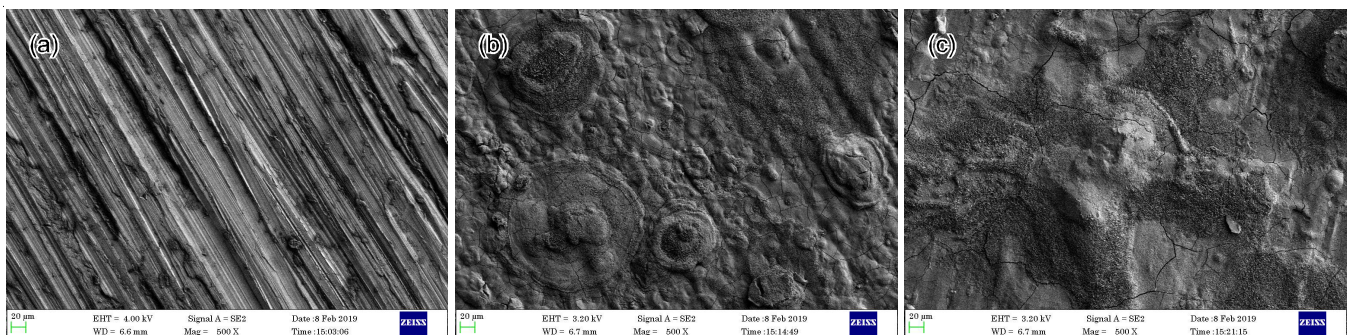
Fig. 10. FE-SEM images of mild steel specimen exposed to (a) blank (b) 8 % of inhibitor concentration (c) only inhibitor
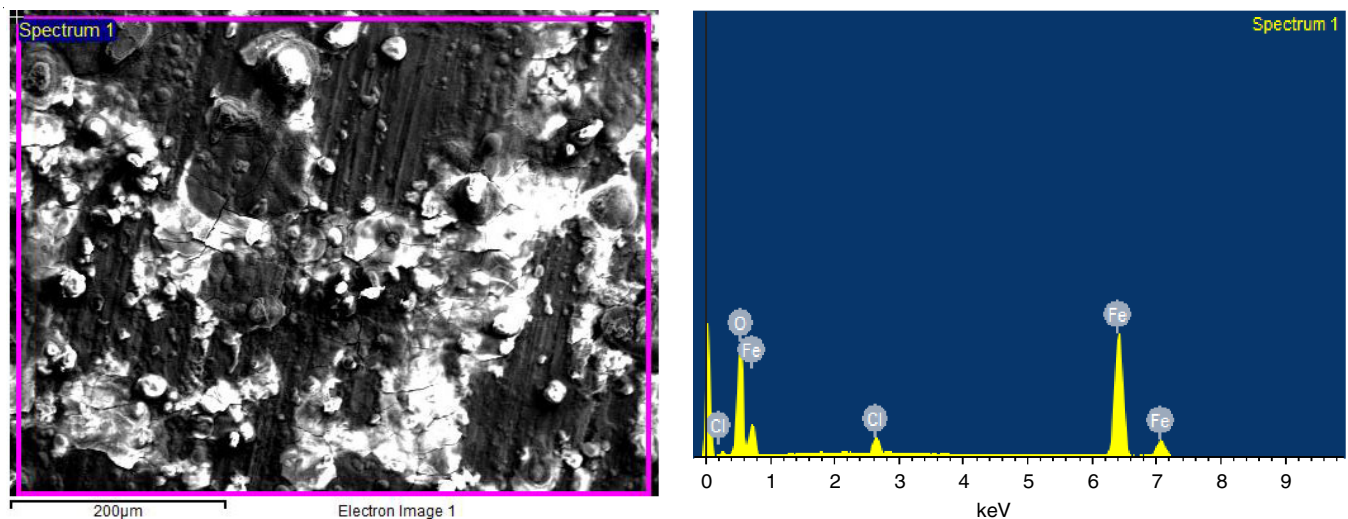
Fig. 11. EDX spectrum of specimen exposed to only inhibitor

were also measured. Interfacial tension is the work done to merge the water drop on the interface. So if the IFT value is less, the surface is more hydrophilic. Here the IFT values obtained for blank, optimum concentration and only inhibitor are 0.98, 2.01 and 2.80 mN/m, respectively. Here, we attribute the inhibition efficiency is because of the adsorption of inhibitor molecules on the metal surface through the lone pair of electrons [63].

Conclusion

Promising results have been obtained from the various studies for *Alstonia schoalris* leaves as pickling inhibitor. It was found that maximum efficiency is shown by an optimum concentration of 8 % and as time of immersion increases inhibition efficiency decreases. From the polarization studies like Tafel and impedance studies showed the inhibitor to be a mixed type. Langmuir adsorption isotherm indicates monolayer adsorption of inhibitor molecules on metal surface, while the values of free energy change indicated that the adsorption is merely physisorption. FTIR showed the functional groups present in the molecule with hetero atoms responsible for high inhibition efficiency. The hetero-atom interacts with the metal surface through their lone pair of electrons and creates a barrier layer and thus inhibiting the rate of corrosion. This facilitates the hydrophilic nature of the inhibitor surface obtained from contact angle measurement. Similarly, negative zeta potential showed the instability of particles in the dispersion medium which aids to the adsorption of particle on the metal surface.

CONFLICT OF INTEREST

The authors declare that there is no conflict of interests regarding the publication of this article.

REFERENCES

1. G. Khan, K.M.S. Newaz, W.J. Basirun, H.B.M. Ali, F.L. Faraj and G.M. Khan, *Int. J. Electrochem. Sci.*, **10**, 6120 (2015).
2. M. Lagrenée, B. Mernari, N. Chaibi, M. Traisnel, H. Vezin and F. Bentiss, *Corros. Sci.*, **30**, 123 (2001);
https://doi.org/10.1016/S0010-938X(00)00076-7.
3. E.E. Oguzie, *Corros. Sci.*, **49**, 1527 (2007);
https://doi.org/10.1016/j.corsci.2006.08.009.
4. A.M. Abdel-Gaber, E. Khamis, H. Abo-ElDahab and S. Adeel, *Mater. Chem. Phys.*, **109**, 297 (2008);
https://doi.org/10.1016/j.matchemphys.2007.11.038.
5. M. Finšgar and J. Jackson, *Corros. Sci.*, **86**, 17 (2014);
https://doi.org/10.1016/j.corsci.2014.04.044.
6. M. Goyal, S. Kumar, I. Bahadur, C. Verma and E.E. Ebenso, *J. Mol. Liq.*, **256**, 565 (2018);
https://doi.org/10.1016/j.molliq.2018.02.045.
7. L. Mardare and L. Benea, *IOP Conf. Series: Mater. Sci. Eng.*, **209**, 012056 (2017);
https://doi.org/10.1088/1757-899X/209/1/012056.
8. U.C. Nwaogu, C. Blawert, N. Scharnagl, W. Dietzel and K.U. Kainer, *Corros. Sci.*, **51**, 2544 (2009);
https://doi.org/10.1016/j.corsci.2009.06.045.
9. E. Vuorinen, E. Kálmán and W. Focke, *Surf. Eng.*, **20**, 281 (2014);
https://doi.org/10.1179/026708404225016481.
10. R.F. da Costa Pereira, E.S.D. de Oliveira, M.A.G. de Andrade Lima and S.L.D. Cezar-Brasil, *Mater. Res.*, **18**, 563 (2015);
https://doi.org/10.1590/1516-1439.341714.
11. A. Devi, A. Singhal and R. Gupta, *Int. J. Environ. Sci.*, **4**, 284 (2013);
12. G. Moretti, G. Quartarone, A. Tassan and A. Zingales, *Br. Corros. J.*, **31**, 49 (1996);
https://doi.org/10.1179/bcj.1996.31.1.49.
13. P.P. Kumari, P. Shetty, S.A. Rao, *Arab. J. Chem.*, **10**, 653 (2017);
https://doi.org/10.1016/j.arabjc.2014.09.005.
14. R.T. Loto, C.A. Loto, O.O. Joseph and G. Olanrewaju, *Results Phys.*, **6**, 305 (2016);
http://dx.doi.org/10.1016/j.rinp.2016.05.013.
15. A.F.S. Abdul Rahiman and S. Sethumanickam, *Arab. J. Chem.*, **10**, S3358 (2017);
https://doi.org/10.1016/j.arabjc.2014.01.016.
16. C. Lai, B. Xie, L. Zou, X. Zheng, X. Ma and S. Zhu, *Results Phys.*, **7**, 3434 (2017);
https://doi.org/10.1016/j.rinp.2017.09.012.
17. R. Karthikaiselvi and S. Subhashini, *J. Assoc. Arab Univ. Basic Appl. Sci.*, **16**, 74 (2014);
https://doi.org/10.1016/j.jaubas.2013.06.002.
18. A. Zarrouk, B. Hammout , H. Zarrok, S.S. Al-Deyab and M. Messali, *Int. J. Electrochem. Sci.*, **6**, 6261 (2011).
19. N.C Subramanyan, B. Sheshadri and S.M. Mayanna, *J. Electrochem. Soc. India*, **42**, 1993, 95-101.
20. P. Shetty, *Surf. Eng. Appl. Electrochem.*, **53**, 587 (2017);
https://doi.org/10.3103/S1068375517060126.
21. C.G.M. de Oliveira, V.W. Faria, G.F. de Andrade, E. D'Elia, M.F. Cabral, B.A. Cotrim, G.O. Resende and F.C. de Souza, Phosphorus, Sulfur, Silicon Rel. Elem., **190**, 1366 (2015);
https://doi.org/10.1080/10426507.2015.1035719.
22. L. Hamadi, S. Mansouri, K. Oulmi and A. Kareche, *Egypt. J. Petrol.*, **27**, 1157 (2018);
https://doi.org/10.1016/j.ejpe.2018.04.004.
23. S.T. Arab and E.A. Noor, *Corrosion*, **49**, 122 (1993);
https://doi.org/10.5006/1.3299206.
24. M.A. Quraishi and R. Sardar, *Corrosion*, **58**, 103 (2002);
https://doi.org/10.5006/1.3277308.
25. P.N. Swathi, K. Rasheeda, S. Samshuddin and V.D.P. Alva, *J. Asian Sci. Res.*, **7**, 301 (2017);
https://doi.org/10.18488/journal.2.2017.78.301.308.
26. A.Y. El Etre and M. Abdallah, *Corros. Sci.*, **42**, 731 (2000);
https://doi.org/10.1016/S0010-938X(99)00106-7.
27. P. Rugmini, A. Anupama, R. Prasad and A. Joseph, *Egypt. J. Petrol.*, **27**, 1067 (2018);
https://doi.org/10.1016/j.ejpe.2018.03.006.
28. M. Ajmal, D. Jamal and M.A. Quraishi, *Anti-Corros. Methods Mater.*, **47**, 77 (2000);
https://doi.org/10.1108/ACMM-12-2013-1338.
29. R. Agarwal and T.K.G. Namboodhiri, *J. Appl. Electrochem.*, **27**, 1265 (1997);
https://doi.org/10.1023/A:1018440105425.
30. F. Bentiss, M. Traisnel and M. Lagrenee, *Corros. Sci.*, **42**, 127 (2000);
https://doi.org/10.1016/S0010-938X(99)00049-9.
31. Y. Yetri and Sukatik, *Orient. J. Chem.*, **33**, 2071 (2017);
http://dx.doi.org/10.13005/ojc/330456
32. E. Baran, A. Cakir and B. Yazici, *Arab. J. Chem.*, (2016);
https://doi.org/10.1016/j.arabjc.2016.06.008.
33. N. Chaubey, V.K. Singh and M.A. Quraishi, *J. Mater. Environ. Sci.*, **7** 2453 (2016).
34. M.T. Majd, S. Asaldoust, G. Bahlakeh, B. Ramezanzadeh and M. Ramezanzadeh, *J. Mol. Liq.*, **284**, 658 (2019);
https://doi.org/10.1016/j.molliq.2019.04.037.
35. R. da Silva Trindade, M.R. dos Santos, R. Fernandes, B. Cordeiro and E. D'Elia, *Green Chem. Lett. Rev.*, **4**, 444 (2017);
https://doi.org/10.1080/17518253.2017.1398354.
36. A. Hamdy and N.Sh. El-Gendy, *Egypt. J. Petrol.*, **22**, 17 (2013);
https://doi.org/10.1016/j.ejpe.2012.06.002.
37. A.Y. EL. Etre, *Corros. Sci.*, **40**, 1845 (1998);
https://doi.org/10.1016/S0010-938X(98)00082-1.
38. S.K. Sharma, A. Peter and I.B. Obot, *J. Anal. Sci. Technol.*, **6**, 26 (2015);
https://doi.org/10.1186/s40543-015-0067-0.
39. P. Sakthivel, P.V. Nirmala, S.Umamaheshwari, A.A. Arul Antony and T. Vasudevan, *Bull. Electrochem. J.*, **15**, 83 (1999).
40. A.D. Arulraj, J. Prabha, R. Deepa, B. Neppolian and V.S. Vasantha, *Mater. Res. Express*, **6**, 036527 (2019);
https://doi.org/10.1088/2053-1591/aaf267.
41. P. Kar, A. Hussein, G. Varkey and G. Singh, *Trans. of MFAI*, **51**, 143 (1996).

42. S. Mohan, J.C. Rani, R.A.L. Sathyanathan, S. Sathiyanarayanan, S. Maruthamuthu and N. Palanisamy, Evaluation of *Nerium oderum*, *Lantana camara* and Aegle manolos Extracts as Corrosion Inhibitors for Mild Steel in 10 % HCl, 10th National Convention of Electrochemistry, pp. 15-17 (2001).

43. J. Arockia Selvi, T.P. Malini, M. Arthanareeswari, P. Kamaraj, R. Mohan Kumar, S.R. Patel and N. Subasree, *Der Pharma Chem.*, **10S**, 1 (2018).

44. M.J. Shanghvi, S.K. Shukla, A.N. Misra, M.R. Pudh and G.N. Mehta, *Bull. Electrochem. J.*, **13**, 358 (1997).

45. A. Smita. G. Verma and G.N. Mehta, *Trans. SAEST*, **33**, 160 (1998).

46. S.J. Zakvi and G.N Mehta, *Trans. SAEST*, **23**, 407 (1987).

47. M. Tezeghdenti, L. Dhouibi and N. Etteyeb, *J. Bio. Tribo. Corros.*, **1**, 16 (2015);
https://doi.org/10.1007/s40735-015-0016-x.

48. C.M. Kliski, J. Radosevic, S. Gudic and C.V. Katalinic, *J. Appl. Electrochem.*, **30**, 823 (2000);
https://doi.org/10.1023/A:1004041530105.

49. G. Matamala, W. Smeltzer and G. Droguett, *Corros. Sci.*, **42**, 1351 (2004);
https://doi.org/10.1016/S0010-938X(99)00137-7.

50. L. Jha, A. Hussain and G. Singh, *Bull. Electrochem.*, **6**, 221 (1991).

51. C.A. Loto and A.I. Mohammed, *Corros. Preven. Contr.*, **4**, 50 (2000).

52. D.A. Winkler, *Metals*, **7**, 553 (2017);
https://doi.org/10.3390/met7120553.

53. C.G. Dariva and A.F. Galio, Corrosion Inhibitors-Principles, Mechanisms and Applications, In: Developments in Corrosion Protection, InTech Open, Chap. 16 (2014).

54. N. Ipek, N. Lior and A. Eklund, *Ironmaking Steelmaking*, **32**, 87 (2005);
https://doi.org/10.1179/174328105X23996.

55. A. Singh, K.R. Ansari, M.A. Quraishi, S. Kayad and P. Banerjee, *New J. Chem.*, **43**, 6303 (2019);
https://doi.org/10.1039/C9NJ00356H.

56. M.T. Alhaffar, S.A. Umoren, I.B. Obot and S.A. Ali, *RSC Adv.*, **8**, 1764 (2018);
https://doi.org/10.1039/C7RA11549K.

57. E.-S.M. Sherif, *Appl. Surf. Sci.*, **292**, 190 (2014);
https://doi.org/10.1016/j.apsusc.2013.11.110.

58. M.H. Othman, A.A.A. Al-Amiery, Y.K. Al-Majedy, A.A. H. Kadhum, A.B. Mohamad and T.S. Gaaz, *Results Phys.*, **8**, 728 (2018);
https://doi.org/10.1016/j.rinp.2017.12.039.

59. A. Peter, S.K. Sharma and I.B. Obot, *J. Anal. Sci. Technol.*, **7**, 26 (2016);
https://doi.org/10.1186/s40543-016-0108-3.

60. P. Kalaria, P. Gheewala, M. Chakraborty and J. Kamath, *Int. J. Res. Ayur. Pharm.*, **3**, 367 (2012).

61. M.A. Quraishi, M.A.W. Khan, M. Ajmal, S. Muralidharan and S. Iyer, *Corrosion*, **53**, 475 (1997);
https://doi.org/10.5006/1.3280490.

62. M. Foss, E. Gulbrandsen and J. Sjöblom, *Corrosion*, **64**, 905 (2008).
https://doi.org/10.5006/1.3294406.

63. D.Q. Huong, T. Duong and P.C. Nam, *ACS Omega*, **4**, 14478 (2019);
https://doi.org/10.1021/acsomega.9b01599.